

NASA

DECLASSIFIED- US: 1688
TAINE TO ROBERTSON MEMO
DATED 9/28/66Declassified by authority of NASA
Classification Change Notices No. 70
Dated ** 10/2/66TECHNICAL MEMORANDUM
X-320STABILITY AND CONTROL CHARACTERISTICS AT A MACH NUMBER
OF 1.41 OF A VARIABLE-SWEEP AIRPLANE CONFIGURATION
CAPABLE OF LOW-LEVEL SUPERSONIC ATTACK - OUTER
WING SWEPT 75° AND 108°

By Ross B. Robinson and Paul W. Howard

Langley Research Center
Langley Field, Va.

GPO PRICE \$ _____

CFSTI PRICE(S) \$ _____

Hard copy (HC) 2.00Microfiche (MF) .50

652 July 65

FACILITY FORM 602

N66 39616

(ACCESSION NUMBER)

27
(PAGES)TMx-320
(NASA CR OR TMX OR AD NUMBER)

(THRU)

(CODE)

(CATEGORY)

NATIONAL AERONAUTICS AND SPACE ADMINISTRATION
WASHINGTON

August 1960

[REDACTED]

NATIONAL AERONAUTICS AND SPACE ADMINISTRATION

TECHNICAL MEMORANDUM X-320

STABILITY AND CONTROL CHARACTERISTICS AT A MACH NUMBER
OF 1.41 OF A VARIABLE-SWEEP AIRPLANE CONFIGURATION

CAPABLE OF LOW-LEVEL SUPERSONIC ATTACK - OUTER

WING SWEEP 75° AND 108° *

By Ross B. Robinson and Paul W. Howard

SUMMARY

An investigation has been conducted in the Langley 4- by 4-foot supersonic pressure tunnel at a Mach number of 1.41 to determine the stability and control characteristics of an airplane configuration capable of low-level supersonic attack. The configuration incorporated a variable-sweep wing, and the investigation was made with outer wing sweep angles of 75° and 108° .

The results indicated that the configuration with the outer wing swept 75° had a stable linear variation of pitching moment with lift and adequate longitudinal control; whereas the 108° swept-wing arrangement had a nonlinear variation of pitching moment with lift and was essentially neutrally stable at positive lift. For both configurations, the directional stability decreased rapidly and the effective dihedral increased with increasing angle of attack. The effects of simulated ground-reflected shock waves for the configuration with the 108° wing indicated that for altitudes less than one-half an airplane length a nose-down pitching moment occurred.

INTRODUCTION

The National Aeronautics and Space Administration is currently investigating airplane configurations capable of long-range low-level supersonic flight. These configurations provide for a fully sweptback wing, a large portion of which is confined within or on top of the fuselage. Several configurations of this type have been investigated

*Title, Unclassified.

[REDACTED]

Declassified by authority of NASA
Classification Change Notices No. 10/2/66

031722-030

at transonic speeds, and some of the results are presented in reference 1. As an extension of the transonic investigation, one of the configurations shown in reference 1 (configuration VIII) has been investigated at supersonic speeds in the Langley 4- by 4-foot supersonic pressure tunnel. The results of tests at a Mach number of 2.01 of the model having a 75° swept wing are presented in reference 2.

The present paper presents the results of tests made at a Mach number of 1.41 of the configuration having wing sweep angles of 75° and 108° .

SYMBOLS

The results are referred to the body-axis system except the lift and drag coefficients which are referred to the stability-axis system. The moment reference point is at a longitudinal station corresponding to 60.5 percent of the body length. (See fig. 1.)

The coefficients and symbols are defined as follows:

| | |
|-------|---|
| C_L | lift coefficient, $\frac{\text{Lift}}{qS}$ |
| C_D | drag coefficient, $\frac{\text{Drag}}{qS}$ |
| C_m | pitching-moment coefficient, $\frac{\text{Pitching moment}}{qSc}$ |
| C_l | rolling-moment coefficient, $\frac{\text{Rolling moment}}{qSb}$ |
| C_n | yawing-moment coefficient, $\frac{\text{Yawing moment}}{qSb}$ |
| C_y | side-force coefficient, $\frac{\text{Side force}}{qS}$ |
| q | free-stream dynamic pressure, lb/sq ft |
| S | reference area, 1.00 sq ft |
| c | reference chord, 1.00 ft |
| b | reference span, 1.00 ft |

DECLASSIFIED

3

| | |
|--------------|--|
| l | model length, measured from nose to engine exit, ft |
| h | distance from model reference line to shock-reflection plane, ft |
| M | free-stream Mach number |
| α | angle of attack, deg |
| β | angle of sideslip, deg |
| δ_h | horizontal-tail deflection, positive when leading edge is up, deg |
| L/D | lift-drag ratio, C_L/C_D |
| $C_{n\beta}$ | directional-stability parameter, $\frac{\partial C_n}{\partial \beta}$, per deg |
| $C_{l\beta}$ | effective-dihedral parameter, $\frac{\partial C_l}{\partial \beta}$, per deg |
| $C_{Y\beta}$ | side-force parameter, $\frac{\partial C_Y}{\partial \beta}$, per deg |

MODEL AND APPARATUS

Details of the model are shown in figure 1. The model with the outer wing panel swept 75° was identical to the configuration of reference 2 having faired inlets and the modified vertical tail. The arrangement with the outer wing panel swept 108° was the same fuselage-tail combination with the wing in the maximum swept position. All tests were made with 0.10-inch-wide transition strips of No. 80 carborundum grains affixed 2 inches behind the fuselage nose and at the 10-percent-chord stations of the wing and tail surfaces.

The model was mounted in the tunnel on a remote-controlled rotary sting. Six-component force and moment measurements were made through the use of an internal strain-gage balance.

DECLASSIFIED



TESTS, CORRECTIONS, AND ACCURACY

The test conditions were as follows:

| | |
|---|--------------------|
| Mach number | 1.41 |
| Stagnation temperature, °F | 100 |
| Stagnation pressure, lb/sq in. | 10 |
| Reynolds number, based on $c = 1.00$ ft | 2.99×10^6 |

The stagnation dewpoint was maintained sufficiently low (-25° F or less) so that no condensation effects were encountered in the test section.

Tests were made for an angle-of-attack range of about -6° to 13° at $\beta \approx 0^\circ$ and for a sideslip range of -6° to 12° at nominal angles of attack of 0° , 4° , and 8° .

The angles of attack and sideslip were corrected for the deflection of the balance and sting under load. The base pressure was measured and the drag force was adjusted to a base pressure equal to free-stream static pressure.

The estimated accuracy of the individual measured quantities based on the repeatability of the results is as follows:

| | |
|----------------------------|--------------|
| C_L | ± 0.0020 |
| C_D | ± 0.0003 |
| C_m | ± 0.0010 |
| C_{l_i} | ± 0.0002 |
| C_n | ± 0.0002 |
| C_Y | ± 0.0003 |
| α , deg | ± 0.2 |
| β , deg | ± 0.2 |
| δ_h , deg | ± 0.1 |

DISCUSSION

75° Swept-Wing Configuration

The longitudinal characteristics of the 75° swept-wing configuration for various horizontal-tail deflections (fig. 2) were similar to those obtained at $M = 2.01$ (ref. 2). A linear variation of C_m with



C_L for positive values of C_L and an average static margin of about 16 percent c are indicated for the moment reference point used. Although the trimming requirements are increased by the small negative value of C_m at $C_L = 0$, deflection of the horizontal tail should provide adequate longitudinal control. The maximum untrimmed value of L/D was about 5.7 and occurred at a lift coefficient of about 0.4. Deflection of the horizontal tail resulted in the decreased lift, increased drag, and reduced L/D , characteristics typical of tail-rearward airplanes.

As is characteristic of low-tail airplanes, the addition of the horizontal tail at $\alpha \approx -0.3^\circ$ produced an increase in the directional stability which became progressively larger with increasing negative deflection (fig. 3). Similar results were indicated for higher values of α with $\delta_h = -5^\circ$ (fig. 4). It is believed that the asymmetry indicated in some of the sideslip data is due in part to asymmetry of the model and in part to flow angularity induced at the tail by the disturbance from the forebody and nacelles.

The effects of angle of attack on the sideslip derivatives for $\delta_h = 0^\circ$ obtained from figure 5 are summarized in figure 6. The results indicate a rapid decrease in the directional-stability parameter $C_{n\beta}$ with increasing angle of attack and an increase in the positive effective-dihedral parameter $-C_{l\beta}$.

108° Swept-Wing Configuration

A nonlinear variation of C_m with C_L and essentially neutral stability for positive values of C_L were indicated for the 108° swept-wing configuration for the moment reference point used (fig. 7). Similar results were obtained at Mach numbers from about 1.0 to 1.2 (ref. 1) for the configuration having the same wing, fuselage, and horizontal tail but with open inlets and a smaller vertical tail. Somewhat less sweep of the outer wing panel or a more forward center-of-gravity location will be required for a longitudinally stable configuration at transonic and low supersonic speeds.

The effects of angle of attack on the sideslip characteristics in figures 8 and 9 are similar to those obtained for the configuration with the outer wing panel swept 75°. A higher value of $C_{n\beta}$ at $\alpha \approx 0^\circ$ was indicated for the 108° swept-wing arrangement, but zero directional stability was obtained at $\alpha \approx 8^\circ$ for both configurations. Somewhat

03:17:30

smaller values of positive effective dihedral were obtained by using the 108° swept wing.

Effect of Simulated Ground-Reflected Shock Waves

The effects of simulated ground-reflected shock waves on the longitudinal characteristics of the 108° swept-wing configuration with $\delta_h = 0^\circ$ are presented in figure 10. These results were obtained by testing the model for a small angle-of-attack range with the center of moments at several constant distances from the tunnel wall in such a way as to simulate operation of the airplane close to the ground. For altitudes of less than one-half an airplane length above the ground, a nose-down pitching moment occurred due to the impingement of the reflected shock on the horizontal tail.

CONCLUDING REMARKS

An investigation has been conducted in the Langley 4- by 4-foot supersonic pressure tunnel to determine the stability and control characteristics of an airplane configuration capable of low-level supersonic attack. The configuration incorporated a variable-sweep wing, and the investigation was made with the outer wing swept back 75° and 108° .

The results indicated that the configuration with the outer wing swept 75° had a stable, linear variation of pitching moment with lift and adequate longitudinal control, whereas the 108° swept-wing arrangement had a nonlinear variation of pitching moment with lift and was essentially neutrally stable at positive lifts. For both configurations, the directional stability decreased rapidly and the effective dihedral increased with increasing angle of attack. The effects of simulated ground-reflected shock waves for the configuration with the 108° wing indicated that for altitudes less than one-half an airplane length a nose-down pitching moment occurred.

Langley Research Center,
National Aeronautics and Space Administration,
Langley Field, Va., June 6, 1960.

[REDACTED]

DECLASSIFIED

7

REFERENCES

1. Bielat, Ralph P., Robins, A. Warner, and Alford, William J., Jr.:
The Transonic Aerodynamic Characteristics of Two Variable-Sweep
Airplane Configurations Capable of Low-Level Supersonic Attack.
NASA TM X-304, 1960.
2. Spearman, M. Leroy, and Robinson, Ross B.: Stability and Control
Characteristics at a Mach Number of 2.01 of a Variable-Sweep
Airplane Configuration Capable of Low-Level Supersonic Attack -
Outer Wing Swept 75°. NASA TM X-310, 1960.

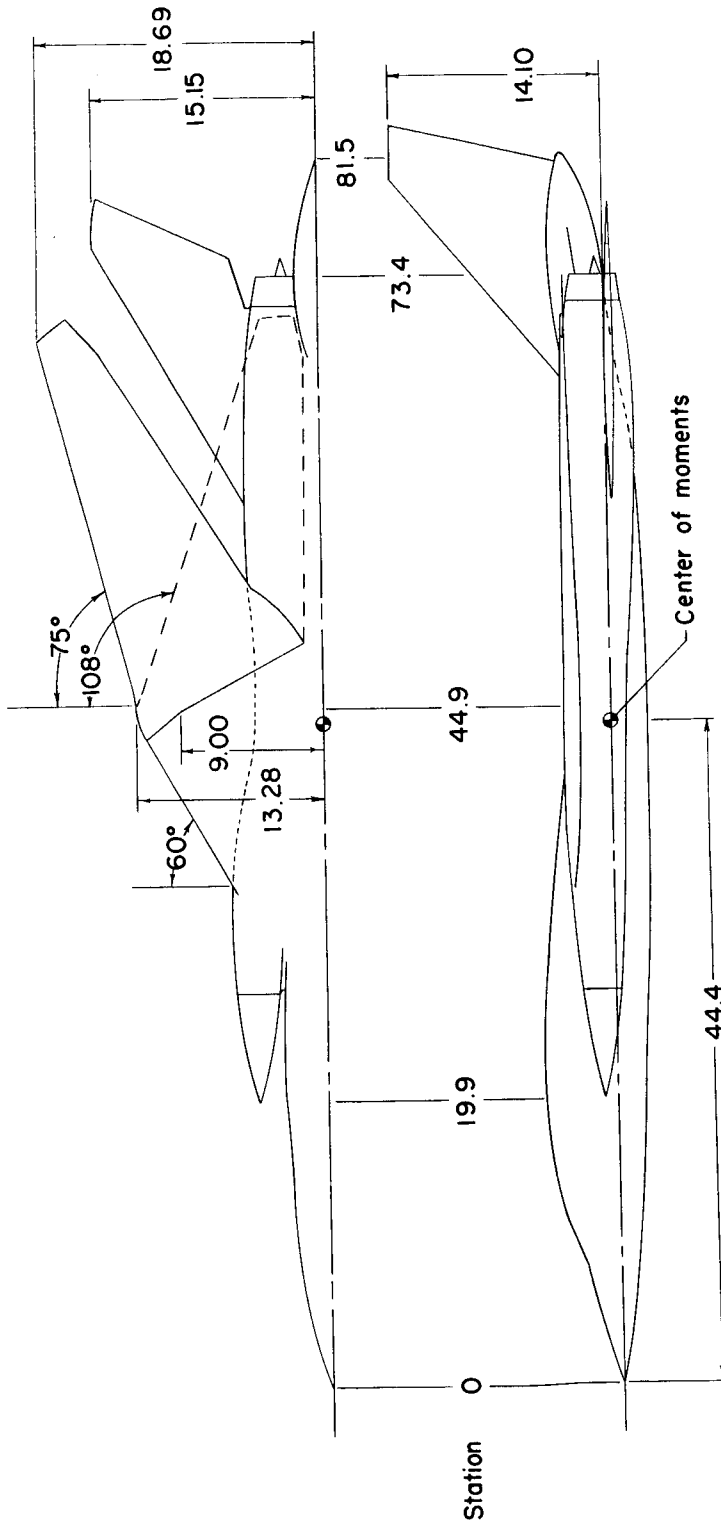
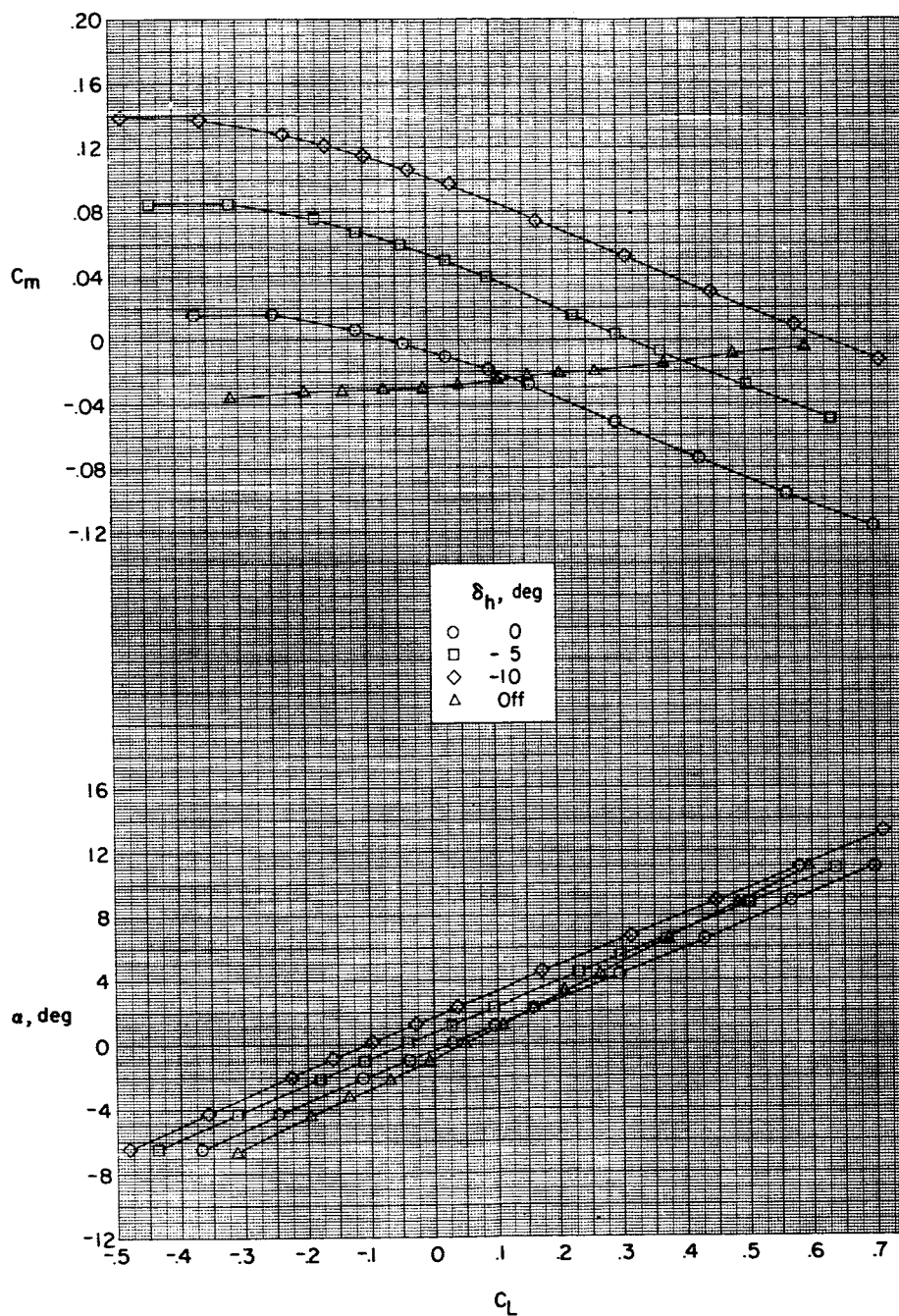


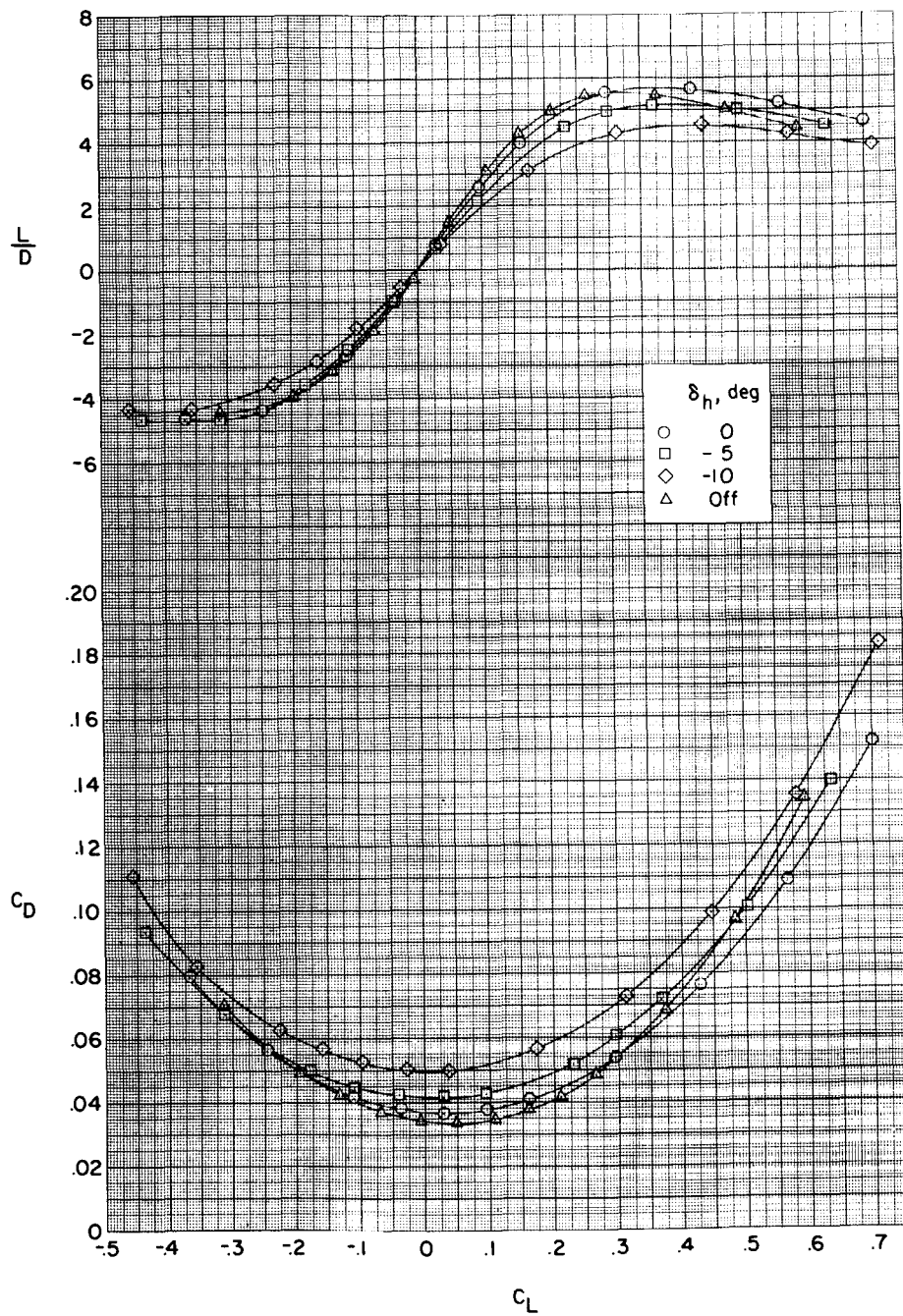
Figure 1.- Details of configuration. All linear dimensions in feet (full scale).



(a) C_m and α against C_L .

Figure 2.- Effect of horizontal-tail deflection on the aerodynamic characteristics in pitch for wing swept 75° .

03 7 10 30



(b) L/D and C_D against C_L .

Figure 2.- Concluded.

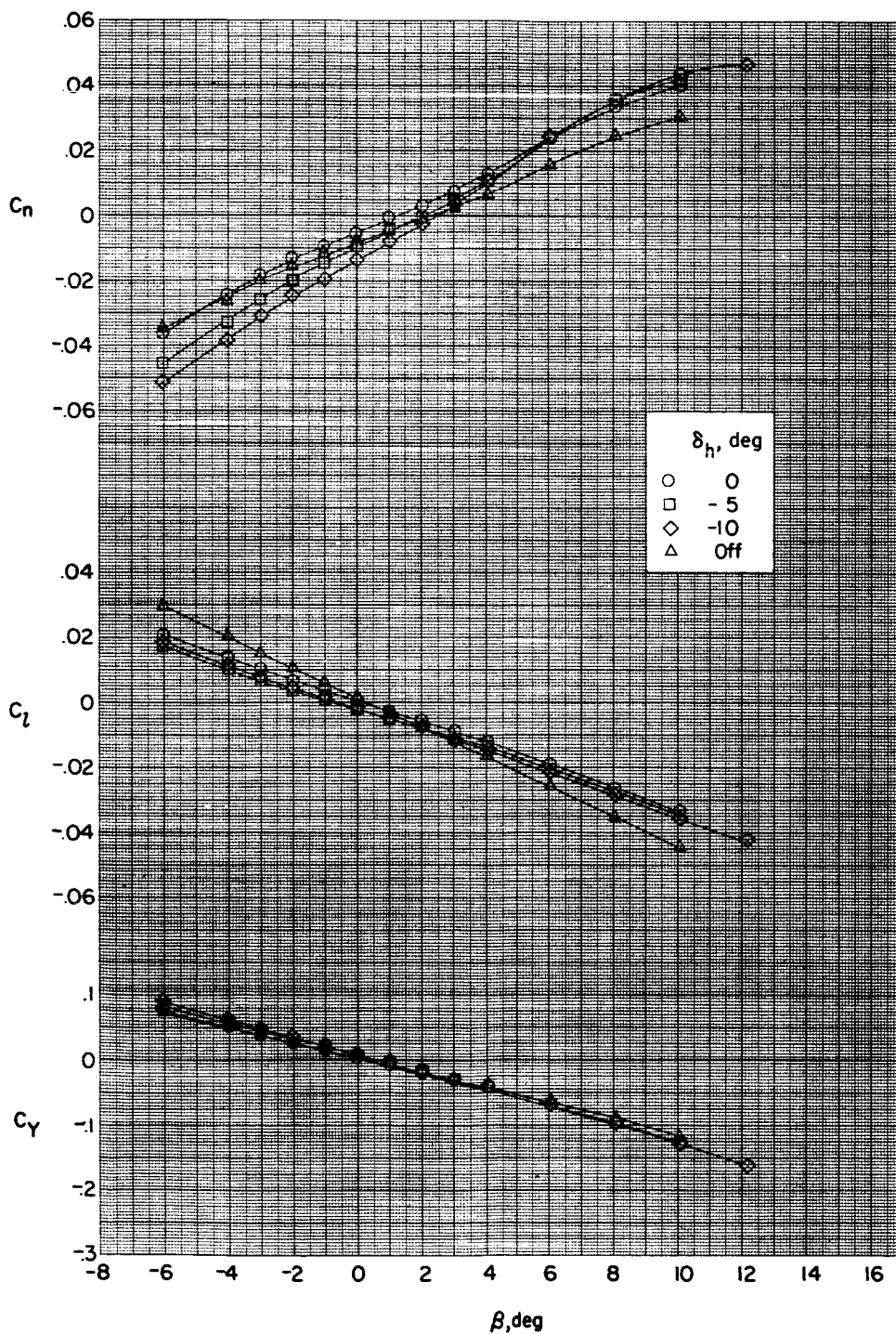
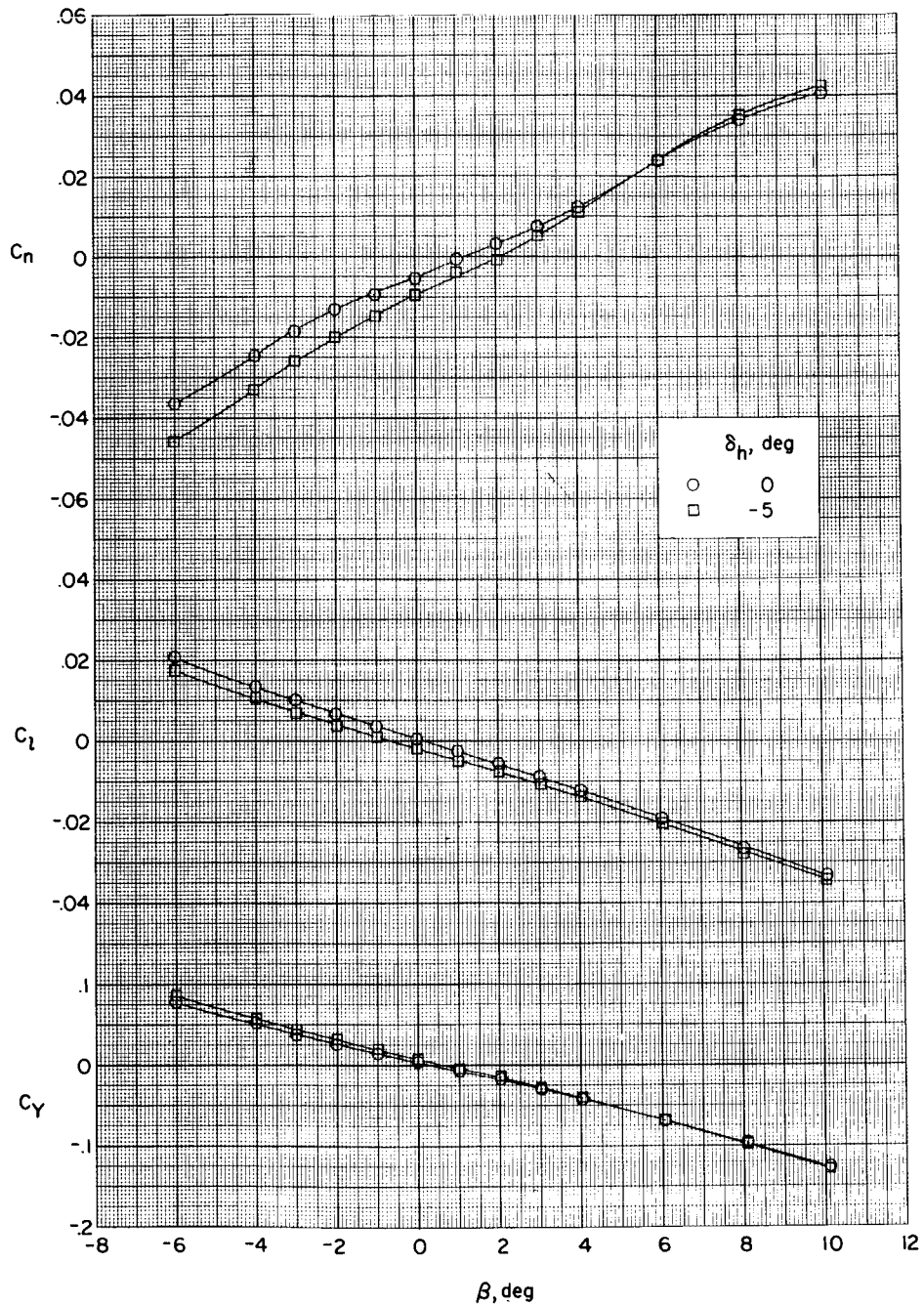
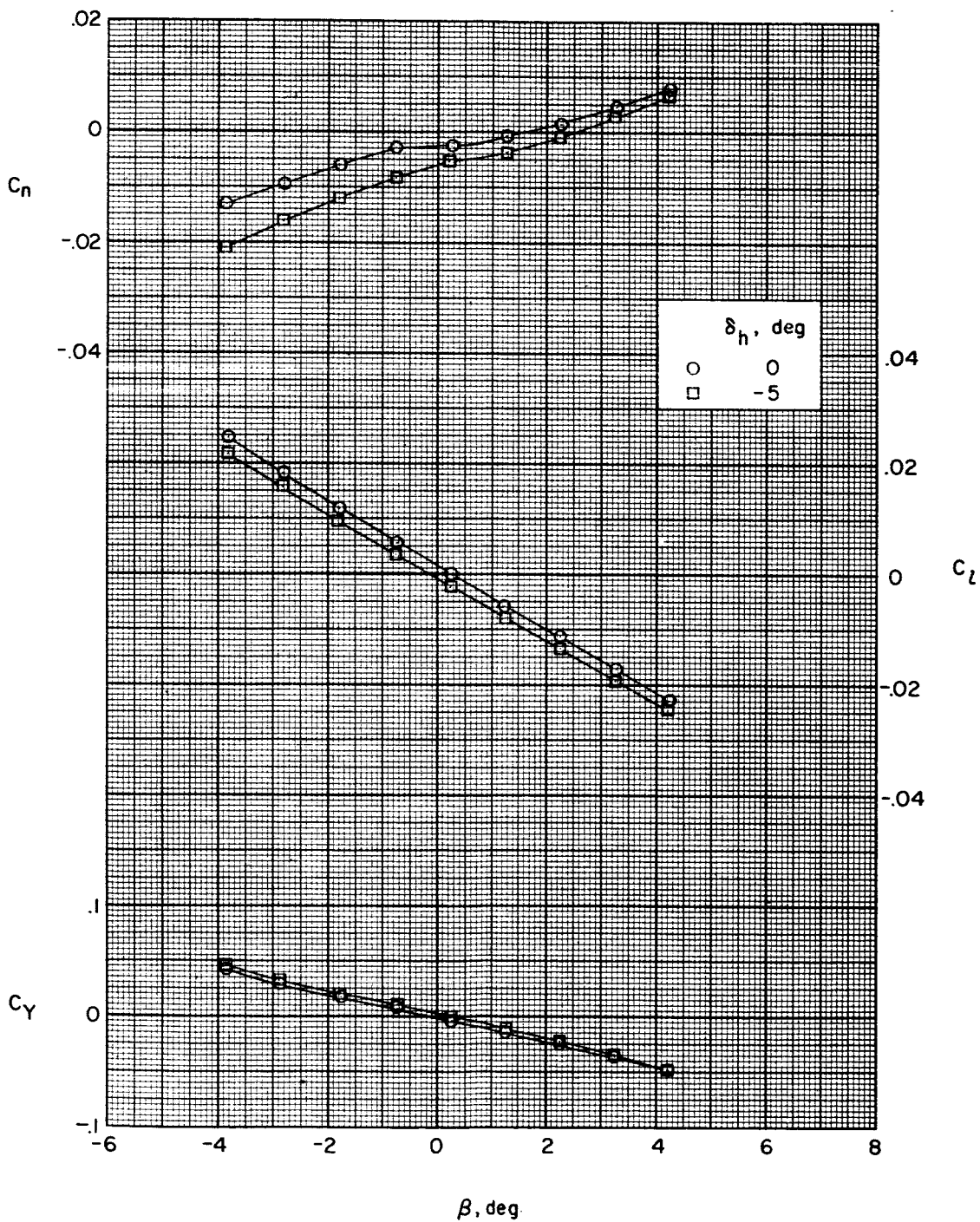


Figure 3.- Effect of horizontal-tail deflection on the aerodynamic characteristics in sideslip at $\alpha \approx -0.3^\circ$ for 75° swept wing.



(a) $\alpha \approx -0.3^\circ$.

Figure 4.- Effect of horizontal-tail deflection on the aerodynamic characteristics in sideslip for various angles of attack for 75° swept wing.



(b) $\alpha \approx 4.3^\circ$.

Figure 4.- Continued.

037-11-6

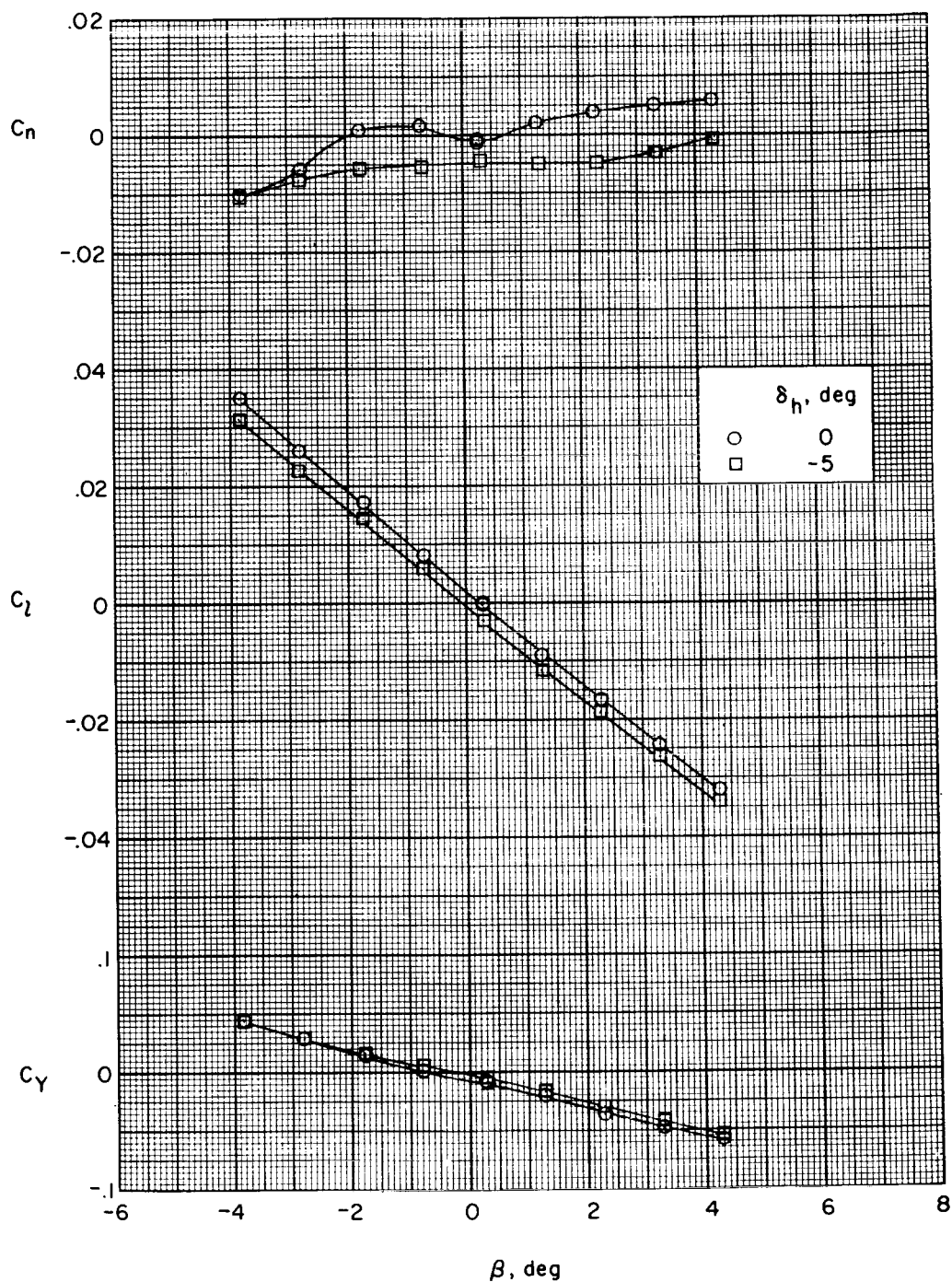
(c) $\alpha \approx 8.7^\circ$.

Figure 4.- Concluded.

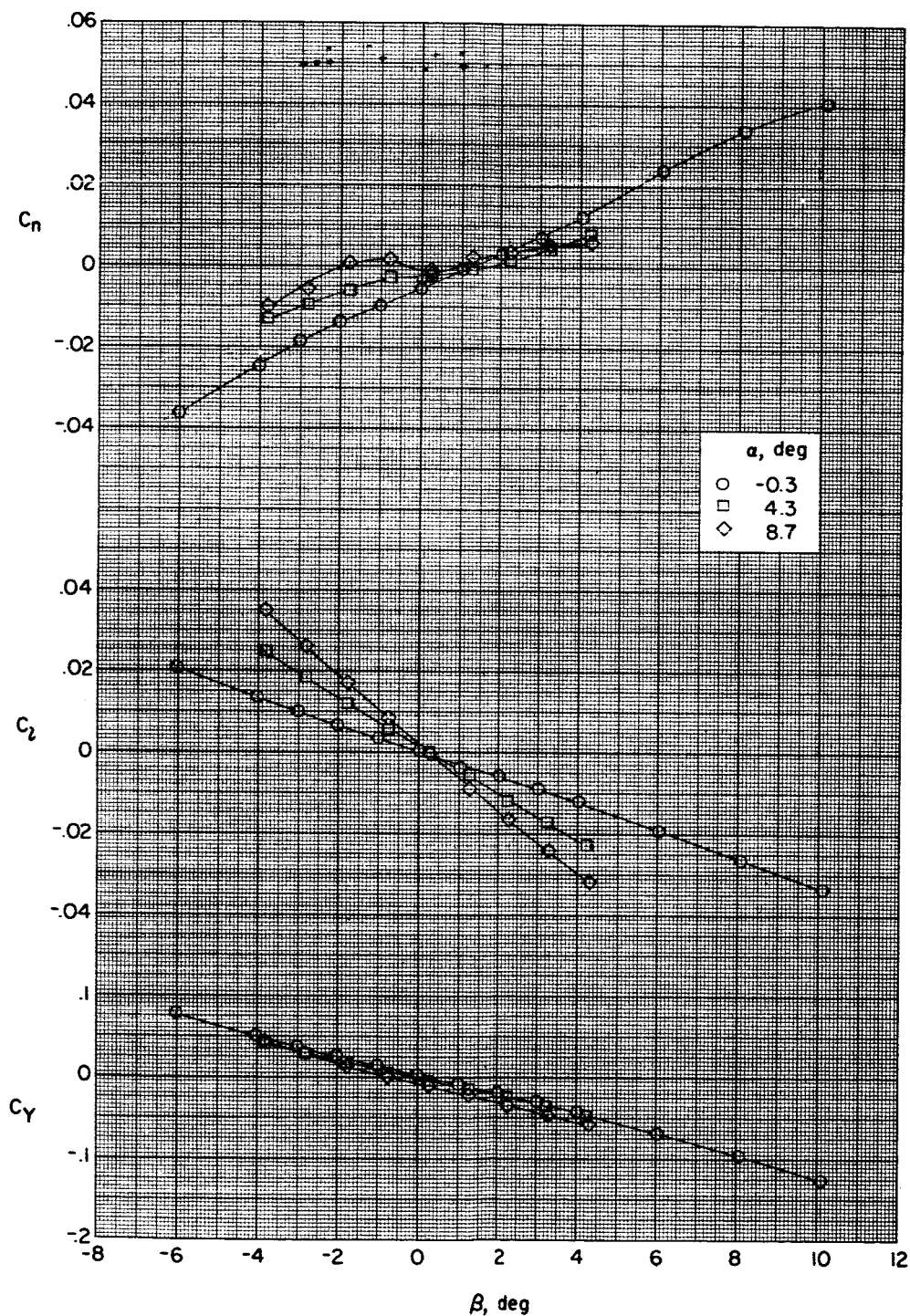


Figure 5.- Effect of angle of attack on the aerodynamic characteristics in sideslip for 75° swept wing; $\delta_h = 0^\circ$.

03 [REDACTED] 00

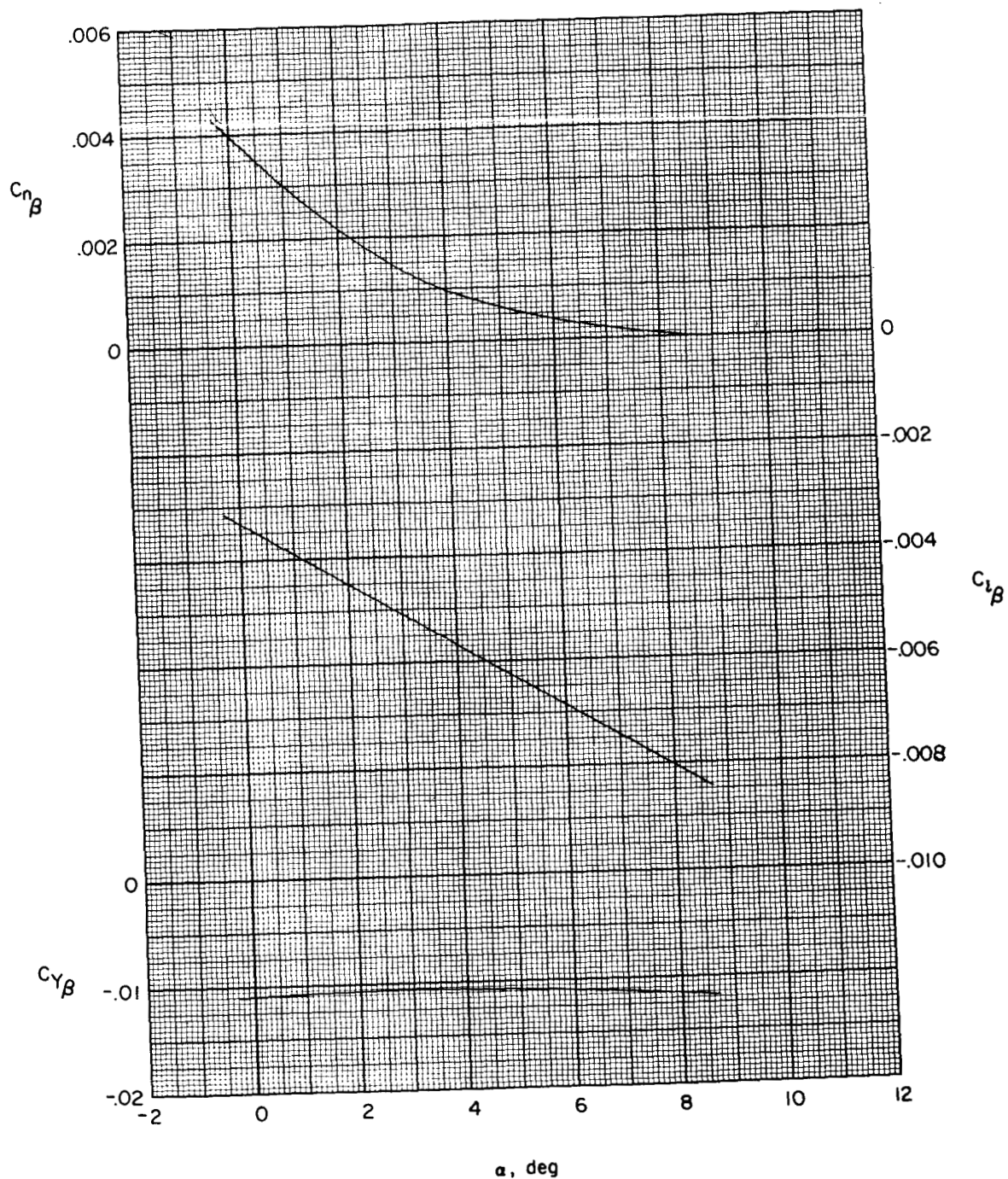
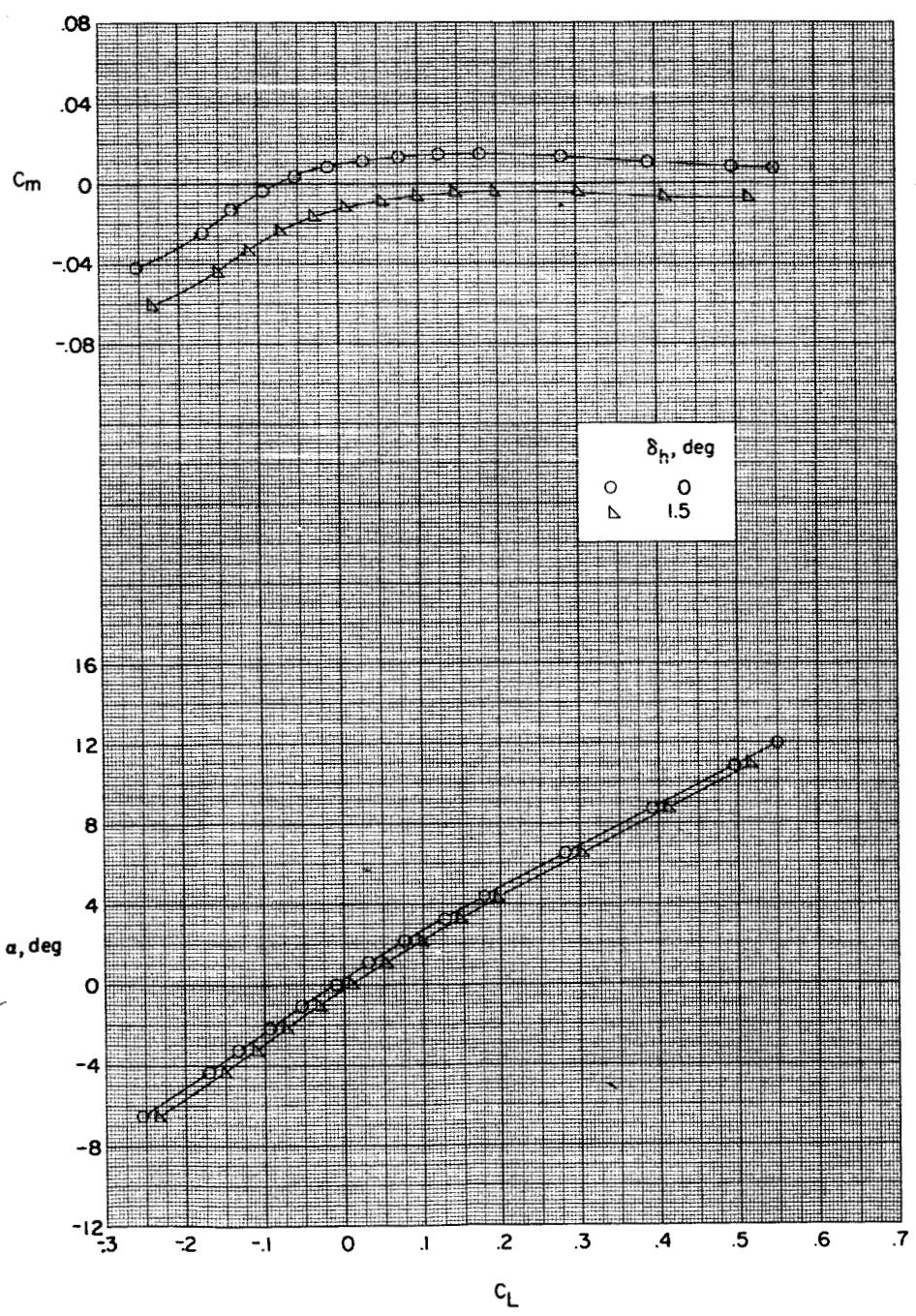


Figure 6.- Variation of sideslip derivatives with angle of attack for 75° swept wing; $\delta_h = 0^\circ$.

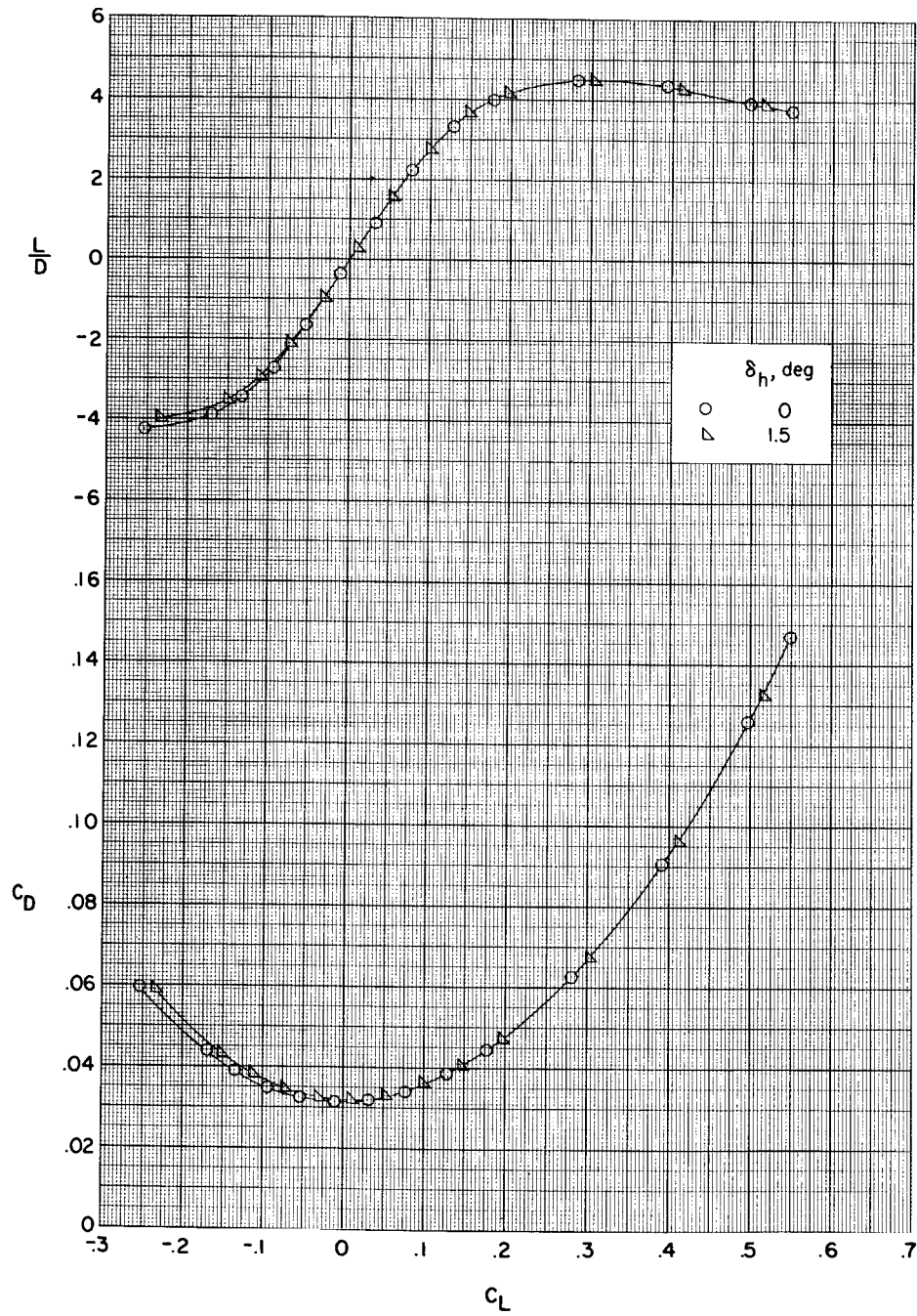
SECRET



(a) C_m and α against C_L .

Figure 7.- Effect of horizontal-tail deflection on the aerodynamic characteristics in pitch for 108° swept wing.

0313 [REDACTED] 030



(b) L/D and C_D against C_L .

Figure 7.- Concluded.

SECRET

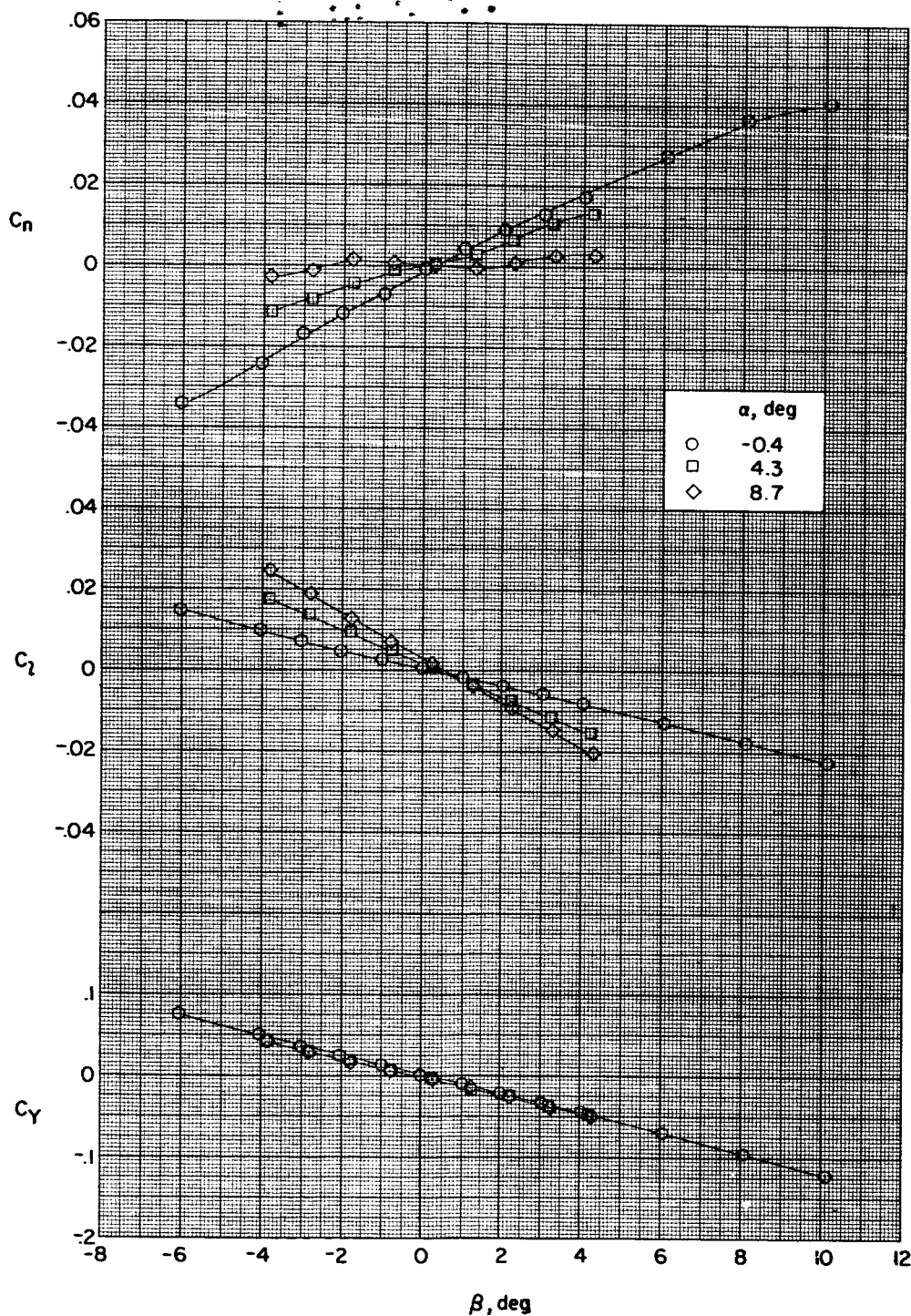


Figure 8.- Effect of angle of attack on the aerodynamic characteristics in sideslip for 108° swept wing; $\delta_h = 0^\circ$.

SECRET

CONFIDENTIAL

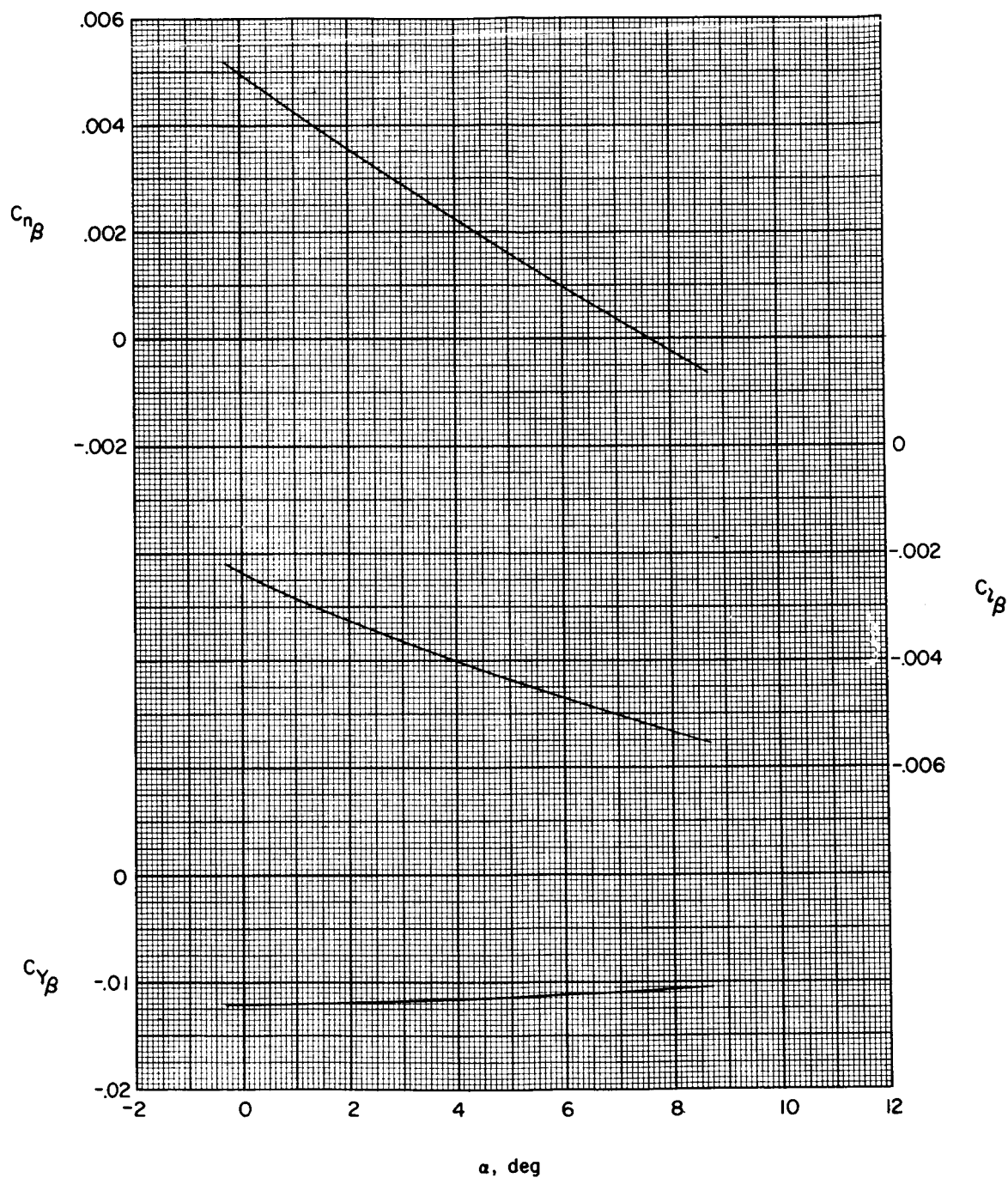
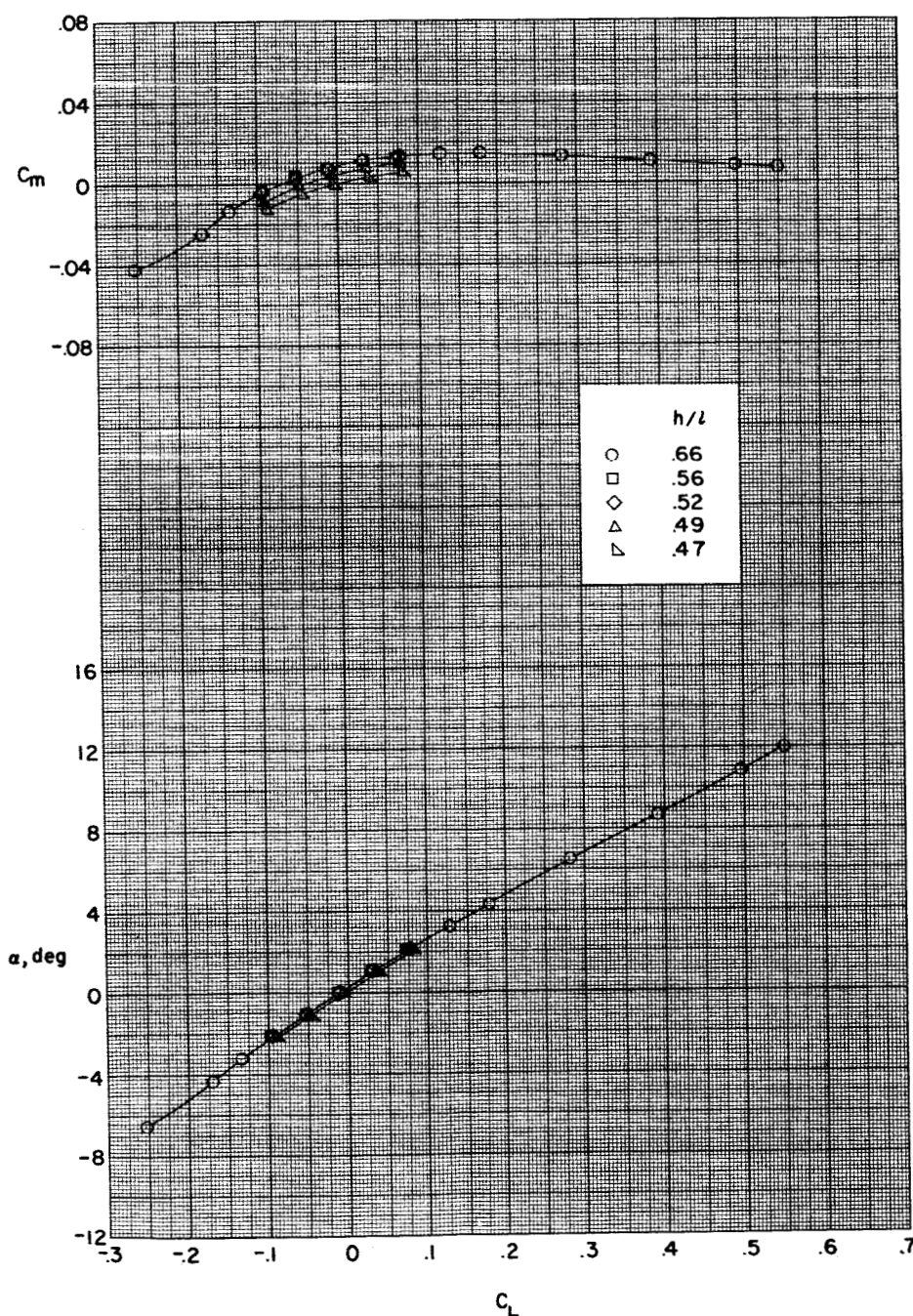


Figure 9.- Variation of sideslip derivatives with angle of attack for 108° swept wing; $\delta_h = 0^\circ$.

SECRET

L-1179

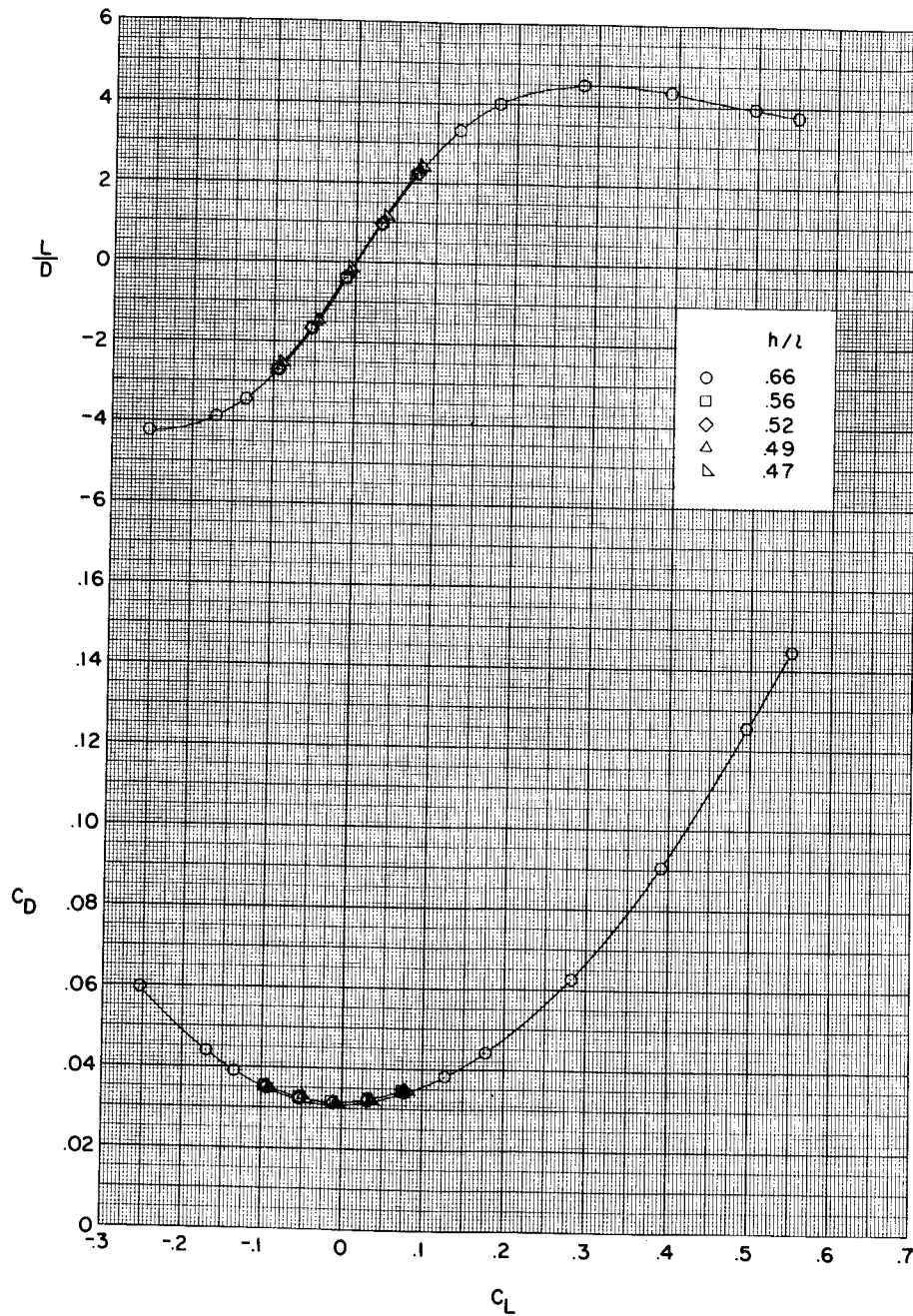


(a) C_m and α against C_L .

Figure 10.- Effect of simulated ground-reflected shock waves on the aerodynamic characteristics in pitch for 108° swept wing; $\delta_h = 0^\circ$.

SECRET

[REDACTED]



(b) L/D and C_D against C_L .

Figure 10.- Concluded.